Pauli graph and finite projective lines/geometries

Michel Planat[a] and Metod Saniga[b]

[a]Institut FEMTO-ST, CNRS, Département LPMO, 32 Avenue del'Observatoire,
F-25044 Besançon, France;
[b]Astronomical Institute, Slovak Academy of Sciences,
SK-05960 Tatranská Lomnica, Slovak Republic

ABSTRACT

The commutation relations between the generalized Pauli operators of N-qudits (i. e., N p-level quantum systems), and the structure of their maximal sets of commuting bases, follow a nice graph theoretical/geometrical pattern. One may identify vertices/points with the operators so that edges/lines join commuting pairs of them to form the so-called Pauli graph $\mathcal{P}_{p^N}$. As per two-qubits ($p = 2$, $N = 2$) all basic properties and partitionings of this graph are embodied in the geometry of the symplectic generalized quadrangle of order two, $W(2)$. The structure of the two-qutrit ($p = 3$, $N = 2$) graph is more involved; here it turns out more convenient to deal with its dual in order to see all the parallels with the two-qubit case and its surmised relation with the geometry of generalized quadrangle $Q(4, 3)$, the dual of $W(3)$. Finally, the generalized adjacency graph for multiple ($N > 3$) qubits/qutrits is shown to follow from symplectic polar spaces of order two/three. The relevance of these mathematical concepts to mutually unbiased bases and to quantum entanglement is also highlighted in some detail.

Keywords: Generalized Pauli operators, Pauli graph, Quantum entanglement, Mutually unbiased bases, Generalized quadrangles, Symplectic polar spaces

1. INTRODUCTION

The structure of commuting/non-commuting relations between N-qudit observables is at the heart of the peculiarities and strangeness of quantum mechanics. Its understanding is central to explain quantum complementarity, quantum entanglement, as well as other conceptual (or practical) issues like no-cloning, quantum teleportation, quantum cryptography and quantum computing, to mention a few.

In Hilbert spaces of prime-power dimension $d = p^N$, p a prime, the $(d^2 - 1)$ generalized Pauli operators organize themselves into $(d+1)$ disjoint sets, each one containing a maximum set of $(d-1)$ mutually commuting operators. In this paper one deals with the Pauli graph $\mathcal{P}_d$ associated with an N-qudit system by regarding the operators as vertices, and joining any pair of commuting ones by an edge. The two-qubit system was studied in much detail in our previous papers[1,2] and found to be related to a well-known finite geometry, namely the generalized quadrangle of order two (see Sec. 2 for details). In this paper, we also analyze the two-qutrit case and give important clues that indicate that the geometry behind the corresponding Pauli graph and/or its dual is that of the symplectic generalized quadrangle of order three, $W(3)$, and/or its dual, $Q(4, 3)$. Finally, we give some hints for generalizations to multiple qudits ($N > 2$), employing symplectic polar spaces of order N as the relevant finite geometries. For more details about the technicalities of the paper, the reader is referred to consult Refs. 2 and 3–6.

Recently, we have found that an important class of finite geometries could be used for coordinatizing some subsets of the Pauli graphs (and, so, some subsets of generalized quadrangles and/or polar spaces) — projective lines defined over finite rings.[7–9] Given an associative ring R with unity and $GL_2(R)$, the general linear group of invertible two-by-two matrices with entries in R, a pair (α, β) is called admissible over R if there exist $\gamma, \delta \in R$

Further author information: (Send correspondence to Michel Planat)
Michel Planat: E-mail: michel.planat@femto-st.fr, Telephone: +33 (0)3 81 85 39 57
Metod Saniga: E-mail: msaniga@astro.sk

such that $\begin{pmatrix} \alpha & \beta \\ \gamma & \delta \end{pmatrix} \in GL_2(R)$. The projective line over R is defined as the set of equivalence classes of ordered pairs $(\varrho\alpha, \varrho\beta)$, where ϱ is a unit of R and (α, β) admissible.[8,9] Such a line carries two non-trivial, mutually complementary relations of neighbor and distant. In particular, its two distinct points X: $(\varrho\alpha, \varrho\beta)$ and Y: $(\varrho\gamma, \varrho\delta)$ are called *neighbor* if $\begin{pmatrix} \alpha & \beta \\ \gamma & \delta \end{pmatrix} \notin GL_2(R)$ and *distant* otherwise. The corresponding graph takes the points as vertices and its edges link any two mutually neighbor points. For R being the finite field $\mathbf{F}_k$, of order k, (the graph of) the projective line lacks any edge, being an independent set of cardinality $k+1$, or a $(k+1)$-coclique. Edges appear only for a line over a ring featuring zero-divisors, and their number is proportional to the number of zero-divisors and/or maximal ideals of the ring concerned (see, e. g., Refs. 7–9 for a comprehensive account of the structure of finite projective ring lines). Projective lines of importance for our model will be the line defined over the (non-commutative) ring of full 2×2 matrices with coefficients in $\mathcal{Z}_2$, as well as the lines defined over three distinct types of rings of order four and characteristic two.[3]

The paper is organized as follows: Secs. 2 and 3 deal, respectively, with the Pauli graphs and the associated geometry of two-qubit and two-qutrit systems and Sec. 4 highlights important geometric-combinatorial clues about arbitrary N-qudits.

2. THE PAULI GRAPH OF TWO-QUBITS

Let us consider the fifteen tensor products $\sigma_i \otimes \sigma_j$, $i, j \in \{1, 2, 3, 4\}$ and $(i, j) \neq (1, 1)$, of Pauli matrices $\sigma_i = (I_2, \sigma_x, \sigma_y, \sigma_z)$, where $I_2 = \begin{pmatrix} 1 & 0 \\ 0 & 1 \end{pmatrix}$, $\sigma_x = \begin{pmatrix} 0 & 1 \\ 1 & 0 \end{pmatrix}$, $\sigma_z = \begin{pmatrix} 1 & 0 \\ 0 & -1 \end{pmatrix}$ and $\sigma_y = i\sigma_x\sigma_z$ and label them as follows $1 = I_2 \otimes \sigma_x$, $2 = I_2 \otimes \sigma_y$, $3 = I_2 \otimes \sigma_z$, $a = \sigma_x \otimes I_2$, $4 = \sigma_x \otimes \sigma_x \ldots$, $b = \sigma_y \otimes I_2, \ldots$, $c = \sigma_z \otimes I_2, \ldots$ Joining two distinct mutually commuting operators by an edge, one obtains the Pauli graph $\mathcal{P}_4$ with incidence matrix as shown in Table 1. The main invariants of $\mathcal{P}_4$ and those of some of its most important subgraphs are listed in Table 2. As it readily follows from Table 1, $\mathcal{P}_4$ is 6-regular and, so, intricately connected with the complete graphs K_n, $n = 5$, 6 or 7. First, one checks that $\mathcal{P}_4 \cong \hat{L}(K_6)$, i. e., it is isomorphic to the complement of line graph of K_6. Next, computing its minimum vertex cover (Table 2), one recovers the Petersen graph $PG \equiv \hat{L}(K_5)$. Finally, $\mathcal{P}_4$ is also found to be isomorphic to the minimum vertex cover of $\hat{L}(K_7)$. Now, we turn to remarkable partitionings/factorizations and the corresponding distinguished subgraphs of $\mathcal{P}_4$.

O_4	1	I_4	1	I_4	1	I_4
1	0	1	0	0	0	0
I_4	1	O_4	0	$\hat{I}_4$	0	$\hat{I}_4$
1	0	0	0	1	0	0
I_4	0	$\hat{I}_4$	1	O_4	0	$\hat{I}_4$
1	0	0	0	0	0	1
I_4	0	$\hat{I}_4$	0	$\hat{I}_4$	1	O_4

Table 1. Structure of the incidence matrix of the two-qubit Pauli graph $\mathcal{P}_4$. The single rows/columns at the reference points a, b and c separate the matrix blocks O_4, I_4 and $\hat{I}_4$.

2.1. The "Fano pencil" FP and the cube CB

We shall first tackle the 7+8 partitioning of the graph which can, for example, be realized by the following subgraphs/subsets: $FP = \langle 1, 2, 3, a, 4, 5, 6 \rangle$ and $CB = \langle b, 7, 8, 9, c, 10, 11, 12 \rangle$ — see Fig. 1. The subgraph FP can also be regarded as a line pencil in the Fano plane[1,10] as well as a hyperplane of $W(2)$;[3] the number of choices for this partitioning is obviously equal to the number of the vertices of the full graph (see Ref. 1 for another choice). It is easy to observe that two vertices on one line of FP map to the third one on the same line, i.e., $1.a = 4$, $2.a = 5$ and $3.a = 6$. The three observables are found to share a common base of 4-dimensional vectors; for this particular choice, the lines in the Fano pencil FP feature unentangled 2-qubit bases. In addition, an edge of CB is mapped to a vertex of FP, e. g., $8.10 = 6$, $8.12 = -4$, etc. In particular there is an Hamiltonian cycle of

G	$\mathcal{P}_4$	$PG \cong MVC$	MS	BP	FP	CB
v	15	10	9	6	7	8
e	45	15	18	9	9	12
$spec(G)$	$\{-3^5,1^9,6\}$	$\{-2^4,1^5,3\}$	$\{-2^4,1^4,4\}$	$\{-3,0^4,3\}$	$\{-2,-1^3,1^2,3\}$	$\{-3,-1^3,1^3,3\}$
$g(G)$	3	5	3	4	3	3
$\kappa(G)$	4	3	3	2	3	2

Table 2. The main invariants of the Pauli graph $\mathcal{P}_4$ and its subgraphs, including its minimum vertex covering MVC isomorphic to the Petersen graph PG. For the remaining symbols, see Refs. 2 and 5.

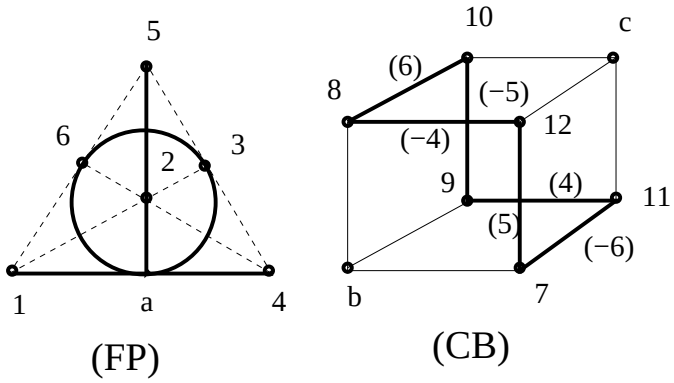

Figure 1. Partitioning of $\mathcal{P}_4$ into a pencil of lines in the Fano plane (FP) and a cube (CB). In FP any two observables on a line map to the third one on the same line. In CB two vertices joined by an edge map to points/vertices in FP. The map is explicitly given for the entangled Hamiltonian path by labels on the corresponding edges.

length 6 (shown with thick lines) in the cube graph CB which features six bases of entangled states. It is worth mentioning here that in Ref. 1 the projective lines over direct product of rings of the type $\mathcal{Z}_2^{\times n}$, $n = 2, 3, 4$, were used to tackle this kind of partitioning. With these lines it was possible to grasp the structure of the two subsets, but not the coupling between them; to get a complete picture required employing a more abstract projective line with a more involved structure.[3]

2.2. The Mermin square MS and the bipartite part BP

We shall focus next on the 9+6 partitioning which can be illustrated, for example, by the subgraphs $BP = \langle 1, 2, 3, a, b, c\rangle$ and $MS = \langle 4, 5, 6, 7, 8, 9, 10, 11, 12\rangle$ — see Fig. 2. The BP part is easily recognized as the bipartite graph $K[3, 3]$, while the MS part is a 4-regular graph. There is a map from the edges of BP to the vertices of MS, and a map from two vertices of a line in MS to the third vertex on the same line. The bases defined by two commuting operators in BP are unentangled. By contrast, operators on any row/column of MS define an entangled base. A square/grid like the MS was used by Mermin[11] — and frequently referred to as a Mermin's square since then — to provide a simple proof of the Kochen-Specker theorem in four dimensions. The proof goes as follows. One observes that the square is polarized in the sense that the product of three operators on any column equals $+I_4$ (the 4×4 identity matrix), while the product of three observables on any row equals $-I_4$. By multiplying all columns and rows one gets $-I_4$. This is, however, not the case for the eigenvalues of the observables; they all equal ± 1 and their corresponding products always yield $+1$ because each of them appears in the product twice; once as the eigenvalue in a column and once as the eigenvalue in a row. The algebraic structure of mutually commuting operators thus contradicts that of their eigenvalues, which furnishes a proof of the Kochen-Specker theorem. The MS set is also recognized as a $(9_2, 6_3)$ configuration for any point is incident with two lines and any line is incident with three points and does not change its shape if we reverse our notation, i. e., join by an edge two mutually non-commuting observables; in graph theoretical terms this means that the MS equals its complement. Last but not least, it needs to be mentioned that the MS configuration represents also the structure of the projective line over the product ring $\mathcal{Z}_2 \times \mathcal{Z}_2$ if we identify the points sets of the two and

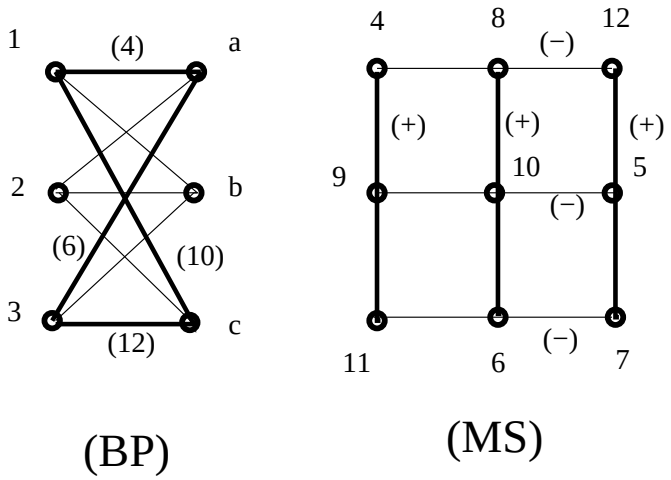

Figure 2. Partitioning of $\mathcal{P}_4$ into an unentangled bipartite graph (BP) and a fully entangled Mermin square (MS). In BP two vertices on any edge map to a point in MS (see the labels of the edges on a selected Hamiltonian path). In MS any two vertices on a line map to the third one. Operators on all six lines carry a base of entangled states. The graph is polarized, i.e., the product of three observables in a row is $-I_4$, while in a column it is $+I_4$.

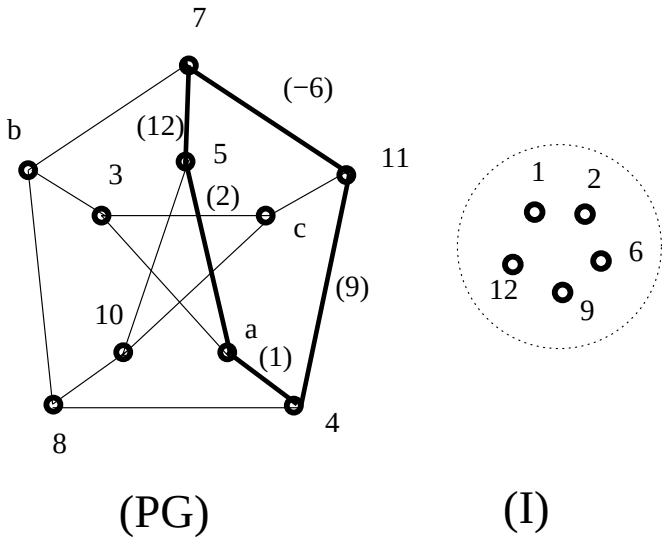

Figure 3. The partitioning of $\mathcal{P}_4$ into an independent set (I) and the Petersen graph (PG), *aka* its minimum vertex cover. The two vertices on an edge of PG correspond/map to a vertex in I (as illustrated by the labels on the edges of a selected Hamiltonian path).

regard edges as joins of mutually *distant* points; it was precisely this fact that motivated our in-depth study of projective ring lines[7,9] and finally led to the discovery of the relevant geometries behind two- and multiple-qubit systems.[1,3,4]

2.3. The Petersen graph PG and the maximum independent set I

The third fundamental partitioning of $\mathcal{P}_4$ comprises a maximum independent set I and the Petersen graph PG.[3] This can be done in six different ways, one of them featuring $I = \langle 1, 2, 6, 9, 12\rangle$ and $PG = \langle 3, a, 4, 5, b, 7, 8, c, 10, 11\rangle$ — see Fig. 3. As in the case of their cousins CB and BP, the Petersen graph PG admits a map of its edges into the vertices of the independent set I.

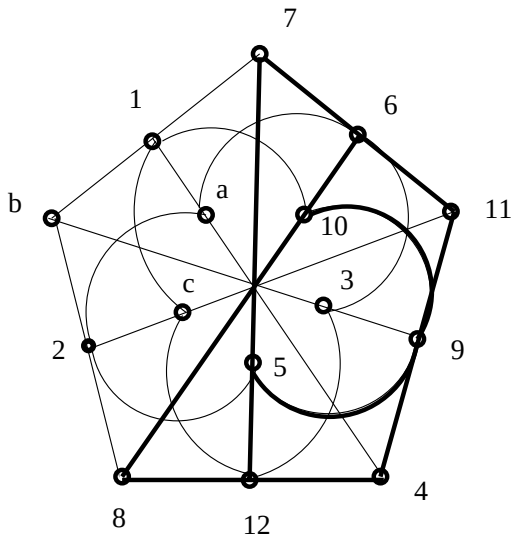

Figure 4. $W(2)$ as the *unique* underlying geometry of two-qubit systems. The Pauli operators correspond to the points and maximally commuting subsets of them to the lines of the quadrangle. Three operators on each line have a common base; six out of fifteen such bases are entangled (the corresponding lines being indicated by boldfacing).

2.4. Finite projective algebraic geometry underlying $\mathcal{P}_4$

2.4.1. $\mathcal{P}_4$ as the generalized quadrangle of order two — $W(2)$

At this point we have dissected $\mathcal{P}_4$ to such an extent that we are ready to show the unique finite projective geometry hidden behind — namely the *generalized quadrangle of order two*, $W(2)$.[3] As already mentioned, $W(2)$ is the simplest thick generalized quadrangle endowed with fifteen points and the same number of lines, where every line features three points and, dually, every point is incident with three lines, and where every point is joined by a line (or, simply, collinear) with other six points.[10,12] These properties can easily be grasped from the drawing of this object, dubbed for obvious reasons the doily, depicted in Fig. 4; here, all the points are drawn as small circles, while lines are represented either by line segments (ten of them), or as segments of circles (the remaining five of them). To recognize in this picture $\mathcal{P}_4$ one just needs to identify the fifteen points of $W(2)$ with our fifteen generalized Pauli operators as explicitly illustrated, with the understanding that *collinear* means *commuting* (and, so, *non*-collinear reads *non*-commuting); the fifteen lines of $W(2)$ thus stand for nothing but fifteen *maximum* subsets of three mutually commuting operators each.

That $W(2)$ is indeed the right projective setting for $\mathcal{P}_4$ stems also from the fact that it gives a nice geometric justification for all the three basic partitionings/factorizations of $\mathcal{P}_4$. To see this, we just employ the fact that $W(2)$ features three distinct kinds of geometric hyperplanes:[12] 1) a *perp*-set ($H_{cl}(X)$), i. e., a set of points collinear with a given point X, the point itself inclusive (there are 15 such hyperplanes); 2) a *grid* (H_{gr}) of nine points on six lines, *aka* a slim generalized quadrangle of order $(2,1)$ (there are 10 such hyperplanes); and 3) an *ovoid* (H_{ov}), i. e., a set of (five) points that has exactly one point in common with every line (there are six such hyperplanes). One then immediately sees[3] that a perp-set is identical with a Fano pencil, a grid answers to a Mermin square and, finally, an ovoid corresponds to a maximum independent set. Because of self-duality of $W(2)$, each of the above introduced hyperplanes has its dual, line-set counterpart. The most interesting of them is the dual of an ovoid, usually called a *spread*, i. e., a set of (five) pairwise disjoint lines that partition the point set; each of six different spreads of $W(2)$ represents such a pentad of mutually disjoint maximally commuting subsets of operators whose associated bases are *mutually unbiased*.[1,13] It is also important to mention a *dual grid*, i. e., a slim generalized quadrangle of order $(1,2)$, having a property that the three operators on any of its nine lines share a base of *un*entangled states. It is straightforward to verify that these lines are defined by the edges of a BP; each of the remaining six lines (fully located in the corresponding/complementary MS) carries a base of *entangled* states (see Fig. 4).

2.4.2. $\mathcal{P}_4$ and the projective line over the full two-by-two matrix ring over $\mathcal{Z}_2$

$W(2)$ is found as a *sub*geometry of many interesting projective configurations and spaces.[10,12] We will now briefly examine a couple of such embeddings of $W(2)$ in order to reveal further intricacies of its structure and, so, to get further insights into the structure of the two-qubit Pauli graph.

We shall first consider an embedding of $W(2)$ in the projective line defined over the ring $\mathcal{Z}_2^{2\times 2}$ of full 2×2 matrices with $\mathcal{Z}_2$-valued coefficients,

$$\mathcal{Z}_2^{2\times 2} \equiv \left\{ \begin{pmatrix} \alpha & \beta \\ \gamma & \delta \end{pmatrix} \mid \alpha, \beta, \gamma, \delta \in \mathcal{Z}_2 \right\}, \tag{1}$$

because it was this projective ring geometrical setting where the relevance of the structure $W(2)$ for two-qubits was discovered.[3] To facilitate our reasonings, we label the matrices of $\mathcal{Z}_2^{2\times 2}$ in the following way

$$\begin{aligned}
&1' \equiv \begin{pmatrix} 1 & 0 \\ 0 & 1 \end{pmatrix},\ 2' \equiv \begin{pmatrix} 0 & 1 \\ 1 & 0 \end{pmatrix},\ 3' \equiv \begin{pmatrix} 1 & 1 \\ 1 & 1 \end{pmatrix},\ 4' \equiv \begin{pmatrix} 0 & 0 \\ 1 & 1 \end{pmatrix},\ 5' \equiv \begin{pmatrix} 1 & 0 \\ 1 & 0 \end{pmatrix},\ 6' \equiv \begin{pmatrix} 0 & 1 \\ 0 & 1 \end{pmatrix}, \\
&7' \equiv \begin{pmatrix} 1 & 1 \\ 0 & 0 \end{pmatrix}, 8' \equiv \begin{pmatrix} 0 & 1 \\ 0 & 0 \end{pmatrix},\ 9' \equiv \begin{pmatrix} 1 & 1 \\ 0 & 1 \end{pmatrix},\ 10' \equiv \begin{pmatrix} 0 & 0 \\ 1 & 0 \end{pmatrix},\ 11' \equiv \begin{pmatrix} 1 & 0 \\ 1 & 1 \end{pmatrix},\ 12' \equiv \begin{pmatrix} 0 & 1 \\ 1 & 1 \end{pmatrix}, \\
&13' \equiv \begin{pmatrix} 1 & 1 \\ 1 & 0 \end{pmatrix},\ 14' \equiv \begin{pmatrix} 0 & 0 \\ 0 & 1 \end{pmatrix},\ 15' \equiv \begin{pmatrix} 1 & 0 \\ 0 & 0 \end{pmatrix},\ 0' \equiv \begin{pmatrix} 0 & 0 \\ 0 & 0 \end{pmatrix},
\end{aligned} \tag{2}$$

and see that $\{1', 2', 9', 11', 12', 13'\}$ are units (i. e., invertible matrices) and $\{0', 3', 4', 5', 6', 7', 8', 10', 14', 15'\}$ are zero-divisors (i. e., matrices with vanishing determinants), with 0' and 1' being, respectively, the additive and multiplicative identities of the ring. Employing the definition of a projective ring line given in Refs. 7 and 8, it is a routine, though a bit cumbersome, task to find out that the line over $\mathcal{Z}_2^{2\times 2}$ is endowed with 35 points whose coordinates, up to left-proportionality by a unit, read as follows

$$\begin{aligned}
&(1',1'),\ (1',2'),\ (1',9'),\ (1',11'),\ (1',12'), (1',13'), \\
&(1',0'),\ (1',3'),\ (1',4'),\ (1',5'),\ (1',6'),\ (1',7'),\ (1',8'),\ (1',10'),\ (1',14'),\ (1',15'), \\
&(0',1'),\ (3',1'),\ (4',1'),\ (5',1'),\ (6',1'),\ (7',1'),\ (8',1'),\ (10',1'),\ (14',1'),\ (15',1'), \\
&(3',4'),\ (3',10'),\ (3',14'),\ (5',4'),\ (5',10'),\ (5',14'),\ (6',4'),\ (6',10'),\ (6',14').
\end{aligned} \tag{3}$$

Next, we pick up two mutually distant points of the line. Given the fact that $GL_2(R)$ act transitively on triples of pairwise distant points,[8] the two points can, without any loss of generality, be taken to be the points $U_0 := (1, 0)$ and $V_0 := (0, 1)$. The points of $W(2)$ are then those points of the line which are either simultaneously distant or simultaneously neighbor to U_0 and V_0. The shared distant points are, in this particular representation, (all the) six points whose both entries are units,

$$\begin{aligned}
&(1',1'),\ (1',2'),\ (1',9'), \\
&(1',11'),\ (1',12'),\ (1',13'),
\end{aligned} \tag{4}$$

whereas the common neighbors comprise (all the) nine points with both coordinates being zero-divisors,

$$\begin{aligned}
&(3',4'),\ (3',10'),\ (3',14'), \\
&(5',4'),\ (5',10'),\ (5',14'), \\
&(6',4'),\ (6',10'),\ (6',14'),
\end{aligned} \tag{5}$$

the two sets thus readily providing a ring geometrical explanation for a $BP + MS$ factorization of the algebra of the two-qubit Pauli operators, Fig. 5, after the concept of mutually *neighbor* is made synonymous with that of mutually *commuting*.[3] To see all the three factorizations within this setting it suffices to notice that the ring $\mathcal{Z}_2^{2\times 2}$ contains as subrings all the *three* distinct kinds of rings of order four and characteristic two, viz. the (Galois) field $\mathbf{F}_4$, the local ring $\mathcal{Z}_2[x]/\langle x^2\rangle$, and the direct product ring $\mathcal{Z}_2 \times \mathcal{Z}_2$,[14] and check that the corresponding lines can be identified with the three kinds of geometric hyperplanes of $W(2)$ as shown in Table 3.[3]

Table 3. Three kinds of the distinguished subsets of the generalized Pauli operators of two-qubits ($\mathcal{P}_4$)) viewed either as the geometric hyperplanes in the generalized quadrangle of order two ($W(2)$) or as the projective lines over the rings of order four and characteristic two residing in the projective line over $\mathcal{Z}_2^{2\times 2}$.

$\mathcal{P}_4$	set of five mutually non-commuting operators	set of six operators commuting with a given one	nine operators of a Mermin's square
$W(2)$	ovoid	perp-set\{reference point}	grid
Proj. Lines over	$\mathbf{F}_4 \cong \mathcal{Z}_2[x]/\langle x^2+x+1\rangle$	$\mathcal{Z}_2[x]/\langle x^2\rangle$	$\mathcal{Z}_2 \times \mathcal{Z}_2 \cong \mathcal{Z}_2[x]/\langle x(x+1)\rangle$

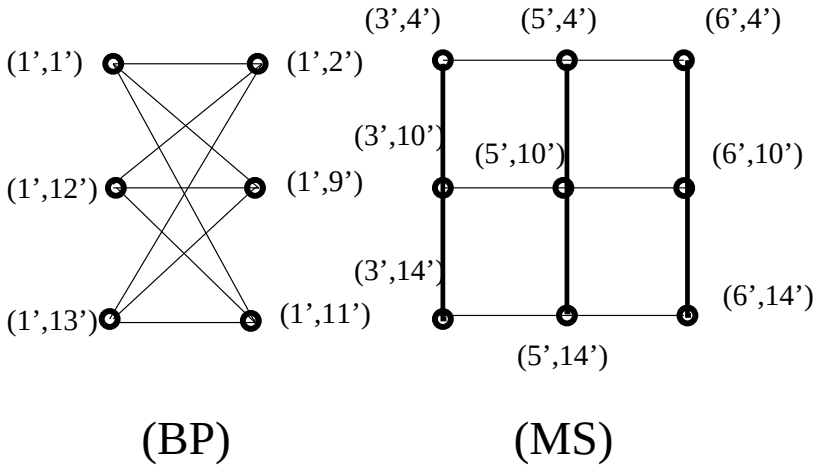

Figure 5. A $BP + MS$ factorization of $\mathcal{P}_4$) in terms of the points of the subconfiguration of the projective line over the full matrix ring $\mathcal{Z}_2^{2\times 2}$; the points of the BP have both coordinates units, whilst those of the MS feature in both entries zero-divisors. The "polarization" of the Mermin square is in this particular ring geometrical setting expressed by the fact that each column/row is characterized by the fixed value of the the first/second coordinate. Compare with Fig. 2.

The other embedding of $W(2)$ is the one into the simplest projective space, $PG(3,2)$, as illustrated in Ref. 2. This embedding is, in fact, a very close ally of the previous one due to a remarkable bijective correspondence between the points of the line over $\mathcal{Z}_2^{2\times 2}$ and the lines of $PG(3,2)$.[15] $W(2)$ and $PG(3,2)$ are identical as the point sets, whilst the fifteen lines of $W(2)$ are so-called totally isotropic lines with respect to a symplectic polarity of $PG(3,2)$ (see Sec. 4).

3. THE PAULI GRAPH OF TWO-QUTRITS

A complete orthonormal set of operators of a single-qutrit Hilbert space is[16]

$$\sigma_I = \{I_3, Z, X, Y, V, Z^2, X^2, Y^2, V^2\}, \quad I = 1, 2, 3, \ldots, 9, \tag{6}$$

where I_3 is the 3×3 unit matrix, $Z = \begin{pmatrix} 1 & 0 & 0 \\ 0 & \omega & 0 \\ 0 & 0 & \omega^2 \end{pmatrix}$, $X = \begin{pmatrix} 0 & 0 & 1 \\ 1 & 0 & 0 \\ 0 & 1 & 0 \end{pmatrix}$, $Y = XZ$, $V = XZ^2$ and $\omega = \exp(2i\pi/3)$. Labelling the two-qutrit Pauli operators as follows $1 = I_3 \otimes \sigma_1$, $2 = I_3 \otimes \sigma_2$, $\cdots$, $8 = I_3 \otimes \sigma_8$, $a = \sigma_1 \otimes I_3$, $9 = \sigma_1 \otimes \sigma_1, \ldots$, $b = \sigma_2 \otimes I_3$, $17 = \sigma_2 \otimes \sigma_1, \ldots$, $c = \sigma_3 \otimes I_3, \ldots$, $h = \sigma_8 \otimes I_2, \ldots$, $72 = \sigma_8 \otimes \sigma_8$, one obtains the incidence matrix of the two-qutrit Pauli graph $\mathcal{P}_9$ as shown in Table 4. Here, $B_8 = \begin{pmatrix} U & \hat{U} \\ \hat{U} & U \end{pmatrix}$ with

$U = \begin{pmatrix} 0 & 0 & 0 & 0 \\ 1 & 0 & 1 & 0 \\ 1 & 0 & 0 & 1 \\ 1 & 1 & 0 & 0 \end{pmatrix}$, $E_8 = \begin{pmatrix} 0_4 & I_4 \\ I_4 & 0_4 \end{pmatrix}$, $F_8 = \begin{pmatrix} I_4 & I_4 \\ I_4 & I_4 \end{pmatrix}$, and 0_4 and I_4 are the 4×4-dimensional all-zero and unit matrix, respectively.

E_8	1	F_8	1	F_8	1	F_8	1	F_8	1	F_8	1	F_8	1	F_8	1	F_8
1	0	1	0	0	0	0	0	0	1	1	0	0	0	0	0	0
F_8	1	E_8	0	B_8	0	B_8	0	B_8	1	F_8	0	$\hat{B}_8$	0	$\hat{B}_8$	0	$\hat{B}_8$
1	0	0	0	1	0	0	0	0	0	0	1	1	0	0	0	0
F_8	0	$\hat{B}_8$	1	E_8	0	$\hat{B}_8$	0	B_8	0	B_8	1	F_8	0	B_8	0	$\hat{B}_8$
1	0	0	0	0	0	1	0	0	0	0	0	0	1	1	0	0
F_8	0	$\hat{B}_8$	0	B_8	1	E_8	0	$\hat{B}_8$	0	B_8	0	$\hat{B}_8$	1	F_8	0	B_8
1	0	0	0	0	0	0	0	1	0	0	0	0	0	0	1	1
F_8	0	$\hat{B}_8$	0	$\hat{B}_8$	0	B_8	1	E_8	0	B_8	0	B_8	0	$\hat{B}_8$	1	F_8
1	1	1	0	0	0	0	0	0	0	1	0	0	0	0	0	0
F_8	1	F_8	0	$\hat{B}_8$	0	$\hat{B}_8$	0	$\hat{B}_8$	1	E_8	0	B_8	0	B_8	0	B_8
1	0	0	1	1	0	0	0	0	0	0	0	1	0	0	0	0
F_8	0	B_8	1	F_8	0	B_8	0	$\hat{B}_8$	0	$\hat{B}_8$	1	E_8	0	$\hat{B}_8$	0	B_8
1	0	0	0	0	1	1	0	0	0	0	0	0	0	1	0	0
F_8	0	B_8	0	$\hat{B}_8$	1	F_8	0	B_8	0	$\hat{B}_8$	0	B_8	1	E_8	0	$\hat{B}_8$
1	0	0	0	0	0	0	1	1	0	0	0	0	1	1	0	1
F_8	0	B_8	0	B_8	0	$\hat{B}_8$	1	F_8	0	$\hat{B}_8$	0	$\hat{B}_8$	0	B_8	1	E_8

Table 4. Structure of the incidence matrix of the two-qutrit Pauli graph $\mathcal{P}_9$

Computing the spectrum $\{-7^{15}, -1^{40}, 5^{24}, 25\}$ one observes that the graph is regular, of degree 25, but not strongly regular. The structure of observables in $\mathcal{P}_9$ is much more involved than in the case of two-qubits although it is still possible to recognize identifiable regular subgraphs. In order to get necessary hints for the geometry behind this system, it necessitates to pass to its dual graph, $\mathcal{W}_9$, i. e., the graph whose vertices are maximally commuting subsets (MCSs) of $\mathcal{P}_9$. To this end, let us first give a complete list of the latter:

$$L_1 = \{1, 5, a, 9, 13, e, 41, 45\}, \quad L_2 = \{2, 6, a, 10, 14, e, 42, 46\}, \quad L_3 = \{3, 7, a, 11, 15, e, 43, 47\},$$
$$L_4 = \{4, 8, a, 12, 16, e, 44, 48\}, \quad M_1 = \{1, 5, b, 17, 21, f, 49, 53\}, \quad M_2 = \{2, 6, b, 18, 22, f, 50, 54\},$$
$$M_3 = \{3, 7, b, 19, 23, f, 51, 55\}, \quad M_4 = \{4, 8, b, 20, 24, f, 52, 56\}, N_1 = \{1, 5, c, 25, 29, g, 57, 61\},$$
$$N_2 = \{2, 6, c, 26, 30, g, 58, 62\}, \quad N_3 = \{3, 7, c, 27, 31, g, 59, 63\}, \quad N_4 = \{4, 8, c, 28, 32, g, 60, 64\},$$
$$P_1 = \{1, 5, d, 33, 37, h, 65, 69\}, \quad P_2 = \{2, 6, d, 34, 38, h, 66, 70\}, \quad P_3 = \{3, 7, d, 35, 39, h, 67, 71\},$$
$$P_4 = \{4, 8, d, 36, 40, h, 68, 72\},$$
$$X_1 = \{9, 22, 32, 39, 45, 50, 60, 67\}, \quad X_2 = \{10, 17, 27, 40, 46, 53, 63, 68\}, \quad X_3 = \{11, 20, 30, 33, 47, 56, 58, 69\},$$
$$X_4 = \{12, 23, 25, 34, 48, 51, 61, 70\}, X_5 = \{13, 18, 28, 35, 41, 54, 64, 71\}, X_6 = \{14, 21, 31, 36, 42, 49, 59, 72\},$$
$$X_7 = \{15, 24, 26, 37, 43, 52, 62, 65\}, X_8 = \{16, 19, 29, 38, 44, 55, 57, 66\},$$
$$Y_1 = \{9, 23, 30, 40, 45, 51, 58, 68\}, \quad Y_2 = \{10, 19, 32, 33, 46, 55, 60, 69\}, \quad Y_3 = \{11, 22, 25, 36, 47, 50, 61, 72\},$$
$$Y_4 = \{12, 17, 26, 39, 48, 53, 62, 67\}, Y_5 = \{13, 20, 27, 34, 41, 56, 63, 70\}, Y_6 = \{14, 23, 28, 37, 42, 51, 64, 65\},$$
$$Y_7 = \{15, 18, 29, 40, 43, 54, 57, 68\}, Y_8 = \{16, 21, 30, 35, 44, 49, 58, 71\},$$
$$Z_1 = \{9, 24, 31, 38, 45, 52, 59, 66\}, \quad Z_2 = \{10, 24, 25, 35, 46, 52, 61, 71\}, \quad Z_3 = \{11, 17, 28, 38, 47, 53, 64, 66\},$$
$$Z_4 = \{12, 18, 31, 33, 48, 54, 59, 69\}, Z_5 = \{13, 19, 26, 36, 41, 55, 62, 72\}, Z_6 = \{14, 20, 29, 39, 42, 56, 57, 67\},$$
$$Z_7 = \{15, 21, 32, 34, 43, 49, 60, 70\}, Z_8 = \{16, 22, 27, 37, 44, 50, 63, 65\}.$$

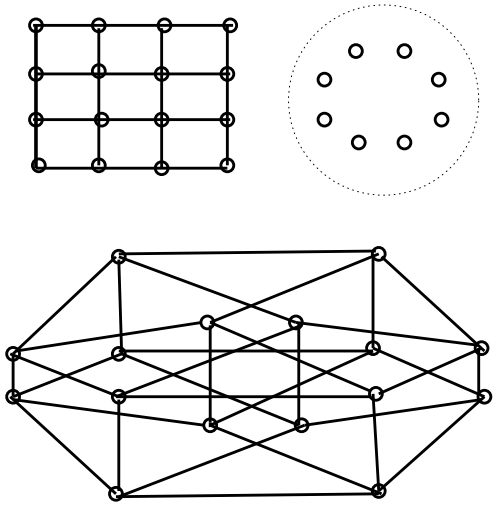

Figure 6. A partitioning of $\mathcal{W}_9$ into a grid (top left), an 8-coclique (top right) and a four-dimensional hypercube (bottom).

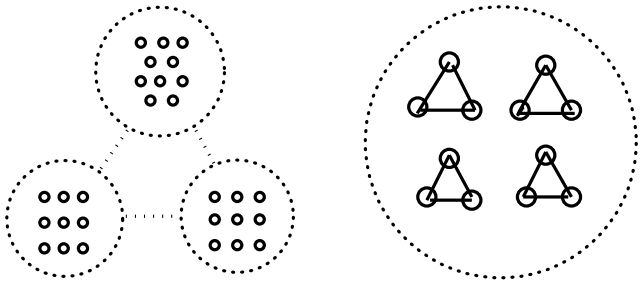

Figure 7. A partitioning of $\mathcal{W}_9$ into a tripartite graph comprising a 10-coclique, two 9-cocliques and a set of four triangles; the lines corresponding to the vertices of a selected triangle intersect at the same observables of $\mathcal{P}_9$ and the union of the latter form a line of $\mathcal{P}_9$.

From there we find that $\mathcal{W}_9$ consists of 40 vertices and has spectrum $\{-4^{15}, 2^{24}, 12\}$, which are the characteristics identical with those of the generalized quadrangle of order three formed by the totally singular points and lines of a parabolic quadric $Q(4,3)$ in $PG(4,3)$.[12] The quadrangle $Q(4,3)$, like its two-qubit counterpart, exhibits all the three kinds of geometric hyperplanes, viz. a slim generalized quadrangle of order (3,1) (a grid), an ovoid, and a perp-set, and these three kinds of subsets can all indeed be found to sit inside $\mathcal{W}_9$. One of the grids is formed by the sixteen lines L_i, M_i, N_i and P_i ($i = 1$, 2, 3 and 4) as illustrated in Fig. 6; the remaining 24 vertices comprise an 8-coclique (X_i, which correspond to mutually unbiased bases), and a four-dimensional hypercube (Y_i and Z_i). Next, one can partition $\mathcal{W}_9$ into an independent set/coclique and the minimum vertex cover using a standard graph software. The cardinality of any independent set is 10 ($= 3^2 + 1$), which means that any such set is an ovoid of $Q(4,3)$.[12] It is easy to verify that, for example, the set $\{L_1, M_2, N_3, P_4, X_3, X_8, Y_4, Y_6, Z_2, Z_7\}$ is an ovoid; given any ovoid/independent set, $Q(4,3)/\mathcal{W}_9$ can be partitioned as shown in Fig. 7. The remaining type of a hyperplane of $\mathcal{W}_9$ is a perp-set, i.e. the set of 12 vertices adjacent to a given ("reference") vertex (Fig. 8); the set of the remaining 27 vertices can be shown to consist of three ovoids which share (altogether and pairwise) just a single vertex — the reference vertex itself. This configuration bears number 99 in a list of graphs with few eigenvalues given in Ref. 17 and can schematically be illustrated in form of a "triangle", with a triangular pattern at its nodes and a 1×2 grid put on its edges; the union of 1×2 grid and a triangle either forms a Mermin-square-type graph M, as already encountered in the two-qubit case, or a quartic graph of another type, denoted as K (see Fig. 8).

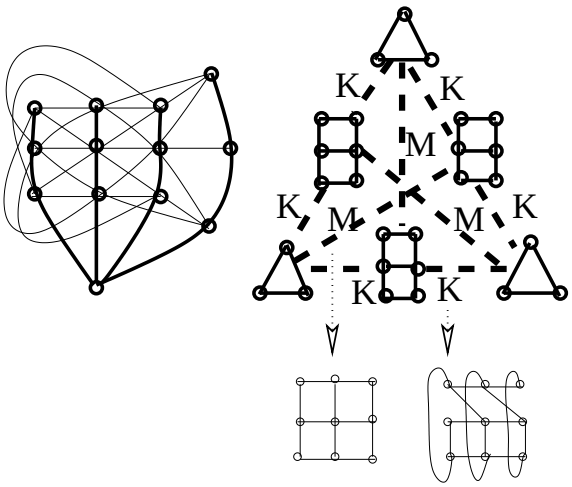

Figure 8. A partitioning of $\mathcal{W}_9$ into a perp-set and a "single-vertex-sharing" union of its three ovoids.

The foregoing observations and facts provide a reliable basis for us to surmise that the geometry behind $\mathcal{W}_9$ is identical with that of $Q(4,3)$. If this is so, then the symplectic generalized quadrangle of order three, $W(3)$, which is the dual of $Q(4,3)$,[12] must underlie the geometry of the Pauli graph $\mathcal{P}_9$. However, the vertex-cardinality of $W(3)$ is 40 (the same as that of $Q(4,3)$), whilst $\mathcal{P}_9$ features as many as 80 points/vertices. Hence, if the geometries of $W(3)$ and $\mathcal{P}_9$ are isomorphic, then there must exits a natural pairing between the Pauli operators such that there exists a bijection between pairs of operators of $\mathcal{P}_9$ and points of $W(3)$. This issue requires, obviously, a much more elaborate analysis, to be the subject of a separate paper.

4. N-QUDIT SYSTEMS AND SYMPLECTIC POLAR SPACES

We have seen that the simplest symplectic generalized quadrangles, viz. $W(2)$ and $W(3)$, are intimately connected with the algebra of generalized Pauli operators of, respectively, two-qubit and two-qutrit systems. Now, it is a well-known fact that symplectic generalized quadrangles $W(q)$, q any power of a prime, are the lowest rank symplectic polar spaces.[12,19,20] This fact is enough to see how to tackle the geometry of multiple (N arbitrary) qudit systems.

A symplectic polar space (see, e. g., Refs. 18–20 for more details) is a d-dimensional vector space over a finite field $\mathbf{F}_q$, $V(d,q)$, carrying a non-degenerate bilinear alternating form. Such a polar space, usually denoted as $W_{d-1}(q)$, exists only if $d = 2N$, with N being its rank. A subspace of $V(d,q)$ is called totally isotropic if the form vanishes identically on it. $W_{2N-1}(q)$ can then be regarded as the space of totally isotropic subspaces of $PG(2N-1,q)$ with respect to a symplectic form, with its maximal totally isotropic subspaces, called also generators G, having dimension $N-1$.

We treat the case $q = 2$, for which this polar space contains

$$|W_{2N-1}(2)| = |PG(2N-1,2)| = 2^{2N} - 1 = 4^N - 1 \tag{7}$$

points and $(2+1)(2^2+1)\ldots(2^N+1)$ generators. A spread S of $W_{2N-1}(q)$ is a set of generators partitioning its points. The cardinalities of a spread and a generator of $W_{2N-1}(2)$ are $|S| = 2^N + 1$ and $|G| = 2^N - 1$, respectively. Finally, it needs to be mentioned that two distinct points of $W_{2N-1}(q)$ are called perpendicular if they are joined by a line; for $q = 2$, there exist $\#_\Delta = 2^{2N-1}$ points that are *not* perpendicular to a given point.

Now, we can identify the Pauli operators of N-qubits with the points of $W_{2N-1}(2)$. If, further, we identify the operational concept "commuting" with the geometrical one "perpendicular," we then readily see that the points lying on generators of $W_{2N-1}(2)$ correspond to maximally commuting subsets (MCSs) of operators and

a spread of $W_{2N-1}(2)$ is nothing but a partition of the whole set of operators into MCSs. Finally, we get that there are 2^{2N-1} operators that do *not* commute with a given operator.

Recognizing $W_{2N-1}(2)$ as the geometry behind N-qubits, we will now turn our attention on the properties of the associated Pauli graphs, $\mathcal{P}_{2^N}$. A strongly regular graph, $\mathrm{srg}(v, D, \lambda, \mu)$, is a regular graph having v vertices and degree D such that any two adjacent vertices are both adjacent to a constant number λ of vertices, and any two distinct non-adjacent vertices are also both adjacent to a constant number μ of vertices. It is known that the adjacency matrix A of any such graph satisfies the following equations[21]

$$AJ = DJ, \qquad A^2 + (\mu - \lambda)A + (\mu - D)I = \mu J, \tag{8}$$

where J is the all-one matrix. Hence, A has D as an eigenvalue with multiplicity one and its other eigenvalues are r (> 0) and l (< 0), related to each other as follows: $r+l = \lambda-\mu$ and $rl = \mu-D$. Strongly regular graphs exhibit many interesting properties.[21] In particular, the two eigenvalues r and l are, except for (so-called) conference graphs, both integers, with the following multiplicities

$$f = \frac{-D(l+1)(D-l)}{(D+rl)(r-l)} \quad \text{and} \quad g = \frac{D(r+1)(D-r)}{(D+rl)(r-l)}, \tag{9}$$

respectively. The N-qubit Pauli graph is strongly regular, and its properties can be inferred from the relation between symplectic polar spaces and partial geometries.

A partial geometry is a more general object than a finite generalized quadrangle. It is finite near-linear space $\{P, L\}$ such that for any point P not on a line L, (i) the number of points of L joined to P by a line equals α, (ii) each line has $(s + 1)$ points, (iii) each point is on $(t + 1)$ lines; this partial geometry is usually denoted as $\mathrm{pg}(s, t, \alpha)$.[6] The graph of $\mathrm{pg}(s, t, \alpha)$ is endowed with $v = (s + 1)\frac{(st+\alpha)}{\alpha}$ vertices, $\mathcal{L} = (t + 1)\frac{(st+\alpha)}{\alpha}$ lines and is strongly regular of the type

$$\mathrm{srg}\left((s+1)\frac{(st+\alpha)}{\alpha}, s(t+1), s-1+t(\alpha-1), \alpha(t+1)\right). \tag{10}$$

The other way round, if a strongly regular graph exhibits the spectrum of a partial geometry, such a graph is called a pseudo-geometric graph. Graphs associated with symplectic polar spaces $W_{2N-1}(q)$ are pseudo-geometric,[21] being

$$\mathrm{pg}\left(q\frac{q^{N-1}-1}{q-1}, q^{N-1}, \frac{q^{N-1}-1}{q-1}\right)\text{-graphs}. \tag{11}$$

Combining these facts with the findings of Sec. 2, we conclude that that N-qubit Pauli graph is of the type given by Eq. (11) for $q = 2$; its basics invariants for a few small values of N are listed in Table 7.

N	v	$\mathcal{L}$	D	r	l	λ	μ	s	t	α
2	15	15	6	1	-3	1	3	2	2	1
3	63	45	30	3	-5	13	15	6	4	3
4	255	153	126	7	-9	61	63	14	8	7

Table 5. Invariants of the Pauli graph $\mathcal{P}_{2^N}$, $N = 2$, 3 and 4, as inferred from the properties of the symplectic polar spaces of order two and rank N. In general, $v = 4^N - 1$, $D = v - 1 - 2^{2N-1}$, $s = 2\frac{2^{N-1}-1}{2-1}$, $t = 2^{N-1}$, $\alpha = \frac{2^{N-1}-1}{2-1}$, $\mu = \alpha(t + 1) = rl + D$ and $\lambda = s - 1 + t(\alpha - 1)) = \mu + r + l$. The integers v and e can also be found from s, t and α themselves.

5. CONCLUSION

We have demonstrated that a particular kind of finite geometries, namely projective ring lines, generalized quadrangles and symplectic polar spaces, are geometries behind finite dimensional Hilbert spaces. A detailed examination of two-qubit (Sec. 2) and two-qutrit (Sec. 3) systems has revealed the fine structure of these geometries and showed how this structure underlies the algebra of the generalized Pauli operators associated with these systems. This study represents a crucial step towards a unified geometric picture, briefly outlined in Sec. 4, encompassing any finite-dimensional quantum system.

ACKNOWLEDGMENTS

This work was partially supported by the Science and Technology Assistance Agency under the contract # APVT–51–012704, the VEGA projects # 2/6070/26 and # 7012 (all from Slovak Republic) and the transnational ECO-NET project # 12651NJ "Geometries Over Finite Rings and the Properties of Mutually Unbiased Bases" (France).

REFERENCES

1. M. Planat, M. Saniga, and M. Kibler, "Quantum entanglement and projective ring geometry," *SIGMA* **2**, Paper 66, 2006.
2. M. Planat and M. Saniga, "On the Pauli graphs of N-qudits," Preprint quant-ph/0701121.
3. M. Saniga, M. Planat, and P. Pracna, "Projective ring line encompassing two qubits," *Theor. Math. Phys.*, submitted; Preprint quant-ph/0611063.
4. M. Saniga and M. Planat, "Multiple qubits as symplectic polar spaces of order two," *Adv. Stud. Theor. Phys.*, submitted; Preprint quant-ph/0612179.
5. F. Harary, *Graph Theory*, Addison-Wesley, Reading, 1972.
6. L. M. Batten, *Combinatorics of Finite Geometries*, Cambridge University Press, Cambridge, 1997 (second edition).
7. M. Saniga, M. Planat, M. R. Kibler, and P Pracna, "A classification of the projective lines over small rings," *Chaos, Solitons and Fractals* **33**, pp. 1095–1102, 2007.
8. A. Blunck and H. Havlicek, "Projective representations I: Projective lines over a ring," *Abh. Math. Sem. Univ. Hamburg* **70**, pp. 287–299, 2000.
9. M. Saniga, M. Planat and P. Pracna, "A classification of the projective lines over small rings. II. Non-commutative case," Preprint math.AG/0706500.
10. B. Polster, *A Geometrical Picture Book*, Springer-Verlag, New York, 1998.
11. N. David Mermin, "Simple unified form for the major no-hidden variable theorems," *Phys. Rev. Lett.* **65**, pp. 3373–3376, 1990.
12. S. E. Payne and J. A. Thas, *Finite Generalized Quadrangles*, Pitman, Boston-London-Melbourne, 1984.
13. J. Lawrence, Č. Brukner, and A. Zeilinger, "Mutually unbiased bases and trinary operators sets for N qubits," *Phys. Rev. A* **65**, pp. 032320–032325, 2002.
14. B. R. McDonald, *Finite Rings With Identity*, Marcel Dekker, New York, 1974.
15. J. A. Thas, "The m-dimensional projective space $S_m(M_n(GF(q)))$ over the total matrix algebra $M_n(GF(q))$ of the $n \times n$ matrices with elements in the Galois field $GF(q)$," *Rend. Mat. Roma* **4**, pp. 459–532, 1971.
16. J. Lawrence, "Mutually unbiased bases and trinary operators sets for N qutrits," *Phys. Rev. A* **70**, 0123021–0123030, 2004.
17. E. R. Van Dam, *Graphs With Few Eigenvalues — An Interplay Between Combinatorics and Algebra*, Thesis, Tilburg University, Center Dissertation Series 20, 1996; Available on-line from http://cage.ugent.be/geometry/Theses/30/evandam.pdf.
18. J. Tits, "Sur la trialité et certains groupes qui s'en déduisent," *Publ. Math. IHES Paris* **2**, pp. 16–60, 1959.
19. P. J. Cameron, "Projective and polar spaces," notes available on-line from http://www.maths.qmul.ac.uk/~pjc/pps/
20. S. Ball, "The geometry of finite fields," *Quaderni Elettronici del Seminario di Geometria Combinatoria* **2E**, 2001; Available on-line from http://www.mat.uniroma1.it/~combinat/quaderni/.
21. F. De Clercq, "(α, β)-geometries from polar spaces," notes available on-line from http://cage.ugent.be/~fdc/brescia_1.pdf.